

Probabilistic computation of Poiseuille flow velocity fields

F. Y. Hunt, J. F. Douglas, and J. Bernal

Citation: *J. Math. Phys.* **36**, 2386 (1995); doi: 10.1063/1.531044

View online: <http://dx.doi.org/10.1063/1.531044>

View Table of Contents: <http://jmp.aip.org/resource/1/JMAPAQ/v36/i5>

Published by the [AIP Publishing LLC](#).

Additional information on *J. Math. Phys.*

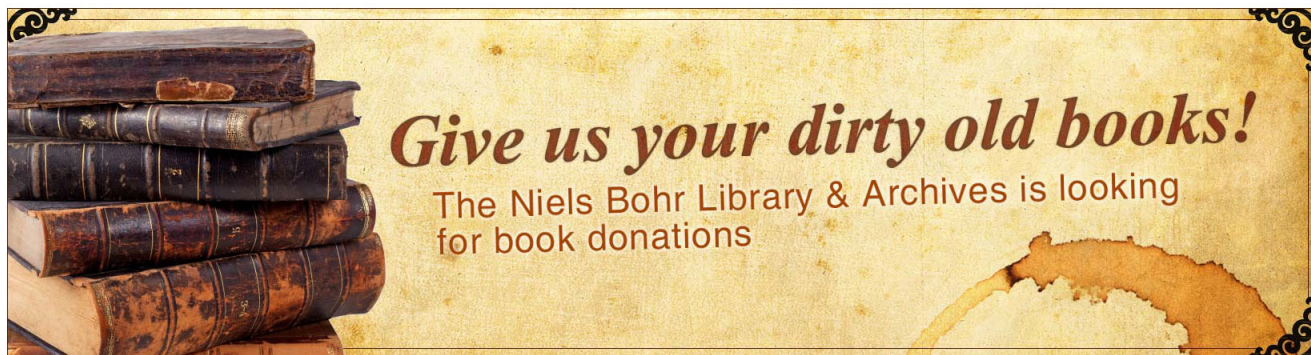
Journal Homepage: <http://jmp.aip.org/>

Journal Information: http://jmp.aip.org/about/about_the_journal

Top downloads: http://jmp.aip.org/features/most_downloaded

Information for Authors: <http://jmp.aip.org/authors>

ADVERTISEMENT



Give us your dirty old books!

The Niels Bohr Library & Archives is looking
for book donations

Probabilistic computation of Poiseuille flow velocity fields

F. Y. Hunt

*Applied and Computational Mathematics Division,
National Institute of Standards and Technology, Gaithersburg, Maryland 20899*

J. F. Douglas

*Polymers Division, National Institute of Standards and Technology,
Gaithersburg, Maryland 20899*

J. Bernal

*Applied and Computational Mathematics Division,
National Institute of Standards and Technology, Gaithersburg, Maryland 20899*

(Received 19 December 1994; accepted for publication 3 January 1995)

Velocity fields for Poiseuille flow through tubes having general cross section are calculated using a path integral method involving the first-passage times of random walks in the interior of the cross sectional domain \mathcal{D} of the pipe. This method is applied to a number of examples where exact results are available and to more complicated geometries of practical interest. These examples include a tube with “fractal” cross section and open channel flows. The calculations demonstrate the feasibility of the probabilistic method for pipe flow and other applications having an equivalent mathematical description (e.g., torsional rigidity of rods, membrane deflection). The example of flow through a fractal pipe shows an extended region of diminished flow velocity near the rough boundary which is similar to the suppressed vibration observed near the boundaries of fractal drums.

I. INTRODUCTION

The problem of calculating fluid flow through and around complex-shaped boundaries has many applications. These applications include porous media problems^{1,2} where the boundaries are not simply connected, screens having complex-shaped holes and hole configurations,³ pipes and streams having undulating channel contour and irregularity in cross sectional shape.^{4,5} In the present article we focus on the idealized problem of Poiseuille flow through pipes having complicated (even “fractal”) cross sections to explore the influence of boundary shape on the flow velocity profile. The numerical calculations of the Poiseuille flow velocity field employ a probabilistic method involving averaging over random walk trajectories. Many boundary value problems involving rough boundaries can be formulated from this point of view⁶ and in the present article we investigate the practical feasibility and accuracy of this type of Monte Carlo method.

Stokes equation for laminar flow in a long tube of uniform cross section (“Poiseuille flow”) simplifies by symmetry to a potential theory boundary value problem. Specifically, if we denote the cross sectional domain defining the tube as \mathcal{D} and the boundary of the the domain as $\partial\mathcal{D}$, then the velocity $v(x)$ at a point x in the interior of \mathcal{D} satisfies the differential equation^{7,8}

$$\eta\nabla^2 v = -\Delta P/L, \quad (1)$$

where ΔP is the (constant) pressure gradient, L is the tube length, and η is the solvent viscosity. Equation (1) assumes that the flow is slow enough that inertial terms in the Navier–Stokes equation can be neglected and that the tube is long enough to neglect end effects.⁹ The velocity of the fluid in the Poiseuille flow vanishes at the rigid pipe boundary so that we must supplement Eq. (1) by the usual “stick” boundary condition

$$v|_{\partial\mathcal{D}}=0. \quad (2)$$

The Poiseuille flow problem thus reduces to the classical Poisson equation with Dirichlet boundary conditions.⁷ Apart from the obvious applications of the Poisson equation to viscometry^{8,10} and technological fluid flow problems where¹¹ tubes of complex boundary shape are involved, we note that there are numerous other applications involving the mathematical equivalent of Eqs. (1) and (2). For example, this equation also describes the torsion of an elastic rod of uniform and simply connected cross section where $v(x)$ corresponds to the stress field and the torsional rigidity of the rod is related to the pipe flux in the “analog” flow problem.¹² A very extensive mathematical and technical literature has been devoted to investigating the relation between the torsional rigidity and the cross sectional shape of the rod^{12–16} and those results are directly transferable to our own problem. Equations (1) and (2) also describe the deflection of clamped membranes¹⁷ (the Prandtl “soap film analogy”) which provides a convenient experimental means of visualizing the velocity (or stress) fields in cases where the boundary shape is complicated. In plasticity theory this equation describes the optimal design of supporting plates having minimum weight¹⁸ and determines an important bound on the yield moments of thin uniformly loaded plates.¹⁹ More recently chemical physics applications have been appreciated. For example, Eqs. (1) and (2) determine the electrostatic free energy of a conducting cavity containing electrolyte in the low salt limit²⁰ and the steady state concentration of a chemical species reacting with the boundary under diffusion limited conditions.²¹ Of course, the solution of the Poisson equation also arises in various electronics and other electrostatic field applications.^{7(c)} Finally, we note applications involving heat transfer through pipes undergoing Poiseuille flow.^{17,22} The heat flux per unit length of a conducting fluid flowing by Poiseuille flow is proportional to ΔP and the volume flux [the integral of $v(x)$ over \mathcal{D}] (Ref. 22) so that Eqs. (1) and (2) have importance in the design of heat exchangers. We conclude that there are many applications of Eqs. (1) and (2) where an easily implementable solution to this problem for shapes with complex boundaries would be valuable.

In the next section we describe our probabilistic method for calculating Poiseuille flow velocity fields and in Sec. III we illustrate the algorithm with examples. We start with square duct flow since this model is analytically tractable and we compare our algorithm with finite element calculations for a notched duct where precise numerical solutions are available for comparison. In the final examples we consider more interesting geometries for the tube cross sections consisting of a fractal, a nonsimply connected flow space, and finally an open channel flow. Some prospects for generalizing the probabilistic algorithm are sketched in the discussion section. Some mathematical aspects of the algorithm are discussed in the Appendices, while the main body of the article emphasizes the numerical implementation of the path integration calculation.

II. PROBABILISTIC COMPUTATION OF THE POISEUILLE FLOW VELOCITY FIELD

It has long been appreciated that potential theory problems can be recast probabilistically through an averaging over random walk paths. Courant *et al.*²³ were the first to have recognized the theoretical possibilities of this approach, while Kakutani²⁴ first discussed an explicit Brownian motion algorithm for the solution of the interior Dirichlet problem for Laplace’s equation. Donsker and Kac²⁴ numerically estimated eigenvalues of Schrödinger’s equation from a path integral representation of the solution. In the 1940’s Wasow²⁵ proved that the mean first-passage time for generalized random walks is a solution of the generalized Poisson equation in the limit of small step sizes, where the random walk approaches a Brownian motion. In particular, this implies that the first-passage time of a symmetric random walk satisfies a discrete Poisson’s equation. Up to a constant of proportionality, the solution of Poisson’s equation at a point x in the interior of \mathcal{D} , is $u(x) = E_x[\tau]$, the average first-passage time of a two dimensional Brownian motion path started at $x \in \mathcal{D}$. This follows from the fact that

$$\nabla^2 u = -2 \quad (3)$$

on the interior of \mathcal{D} and $u=0$ on the boundary $\partial\mathcal{D}$. The velocity field $v(x)$ can therefore be written as

$$v = \Delta P E_x[\tau] / 2 \eta L. \quad (4)$$

Following Wasow, our explicit algorithm is based on approximating Brownian motion by a random walk originating in the interior of \mathcal{D} , and using the fact that the average first-passage time satisfies the discretized form of Eq. (4). A short proof of this fact can be found in the Appendices.

It should be mentioned that Torquato *et al.* have considered random walk calculations of $E_x[\tau]$ in various model porous media as part of their modeling of the rate of diffusion limited reaction rates in these complex geometries and the conductivity of inhomogeneous materials.²⁶ Torquato²⁷ has also derived a rigorous bound on the permeability κ of a porous medium involving an average of $E_x[\tau]$ over the pore space, and the utility of these bounds has recently been considered by Schwartz *et al.*²⁸ In contrast to these previous contributions we are interested in calculating velocity fields by random walk simulation as well as average fluxes and permeabilities.

We consider a rectangle containing the domain \mathcal{D} on which values of the flow velocity are defined. Two dimensional random walks are initiated at each interior position of \mathcal{D} and are terminated when the path reaches the boundary. When the boundaries are relatively simple, detecting when the walk has exited is straightforward. It was desirable, however, to be able to handle the more complex-shaped boundaries encountered in hydrodynamic flow applications (for example, when the cross section is obtained from a micrograph of a porous medium) without doing a time consuming comparison with every point of the boundary each time a random step is taken. We therefore employed a constrained Delaunay triangulation of \mathcal{D} to establish a "roadmap" of the interior by triangulating the rectangle into triangles that were labeled as interior or exterior relative to the boundary of \mathcal{D} .²⁸ The position of the random walk was monitored by identifying the Delaunay triangle that contained it. If a random walk step was taken from an interior to an exterior triangle and was within a step size of a boundary point the step was defined to be an exit. To increase the accuracy a small step size was used. The results of the procedure are shown in the next section where the velocity fields are plotted as a function of the position x within the cross section.

III. ILLUSTRATIVE PROBABILISTIC CALCULATIONS OF THE VELOCITY FIELD

Although many computational techniques (finite element, variational, conformal mapping) exist for calculating the velocity field and flux of Poiseuille flow for complex-shaped boundaries,^{13,15,16} the probabilistic method based on Ref. 14 has the advantage of ease and flexibility of implementation to boundaries of essentially arbitrary shape. This is particularly important in cases where values of v need to be known only approximately. Very little is known in general, however, about the accuracy of these formal probabilistic calculations. Therefore we will consider some simple examples where exact analytic, numerical, and experimental results are known. An early theoretical result of Wasow²⁵ proves that the error of the probabilistic calculation for shapes with smooth boundaries is on the order of the step size of the random walk. Our numerical calculations demonstrate the feasibility of the method. We then consider more complicated shapes where the flexibility of the probabilistic approach should be of practical advantage. The first nontrivial example is a pipe with a fractal boundary similar to one that has been of recent interest as a model porous medium. For example, Stokes equation for a fractal domain has been discussed in a number of articles by Adler and co-workers in both the two and three dimensional cases and they compute an average permeability²⁹ for the corresponding flows. The related boundary value problem of vibration of fractal drums has also been treated recently.^{6(a),30} Finally, technologically motivated flow geometries that arise in automotive applications are discussed.

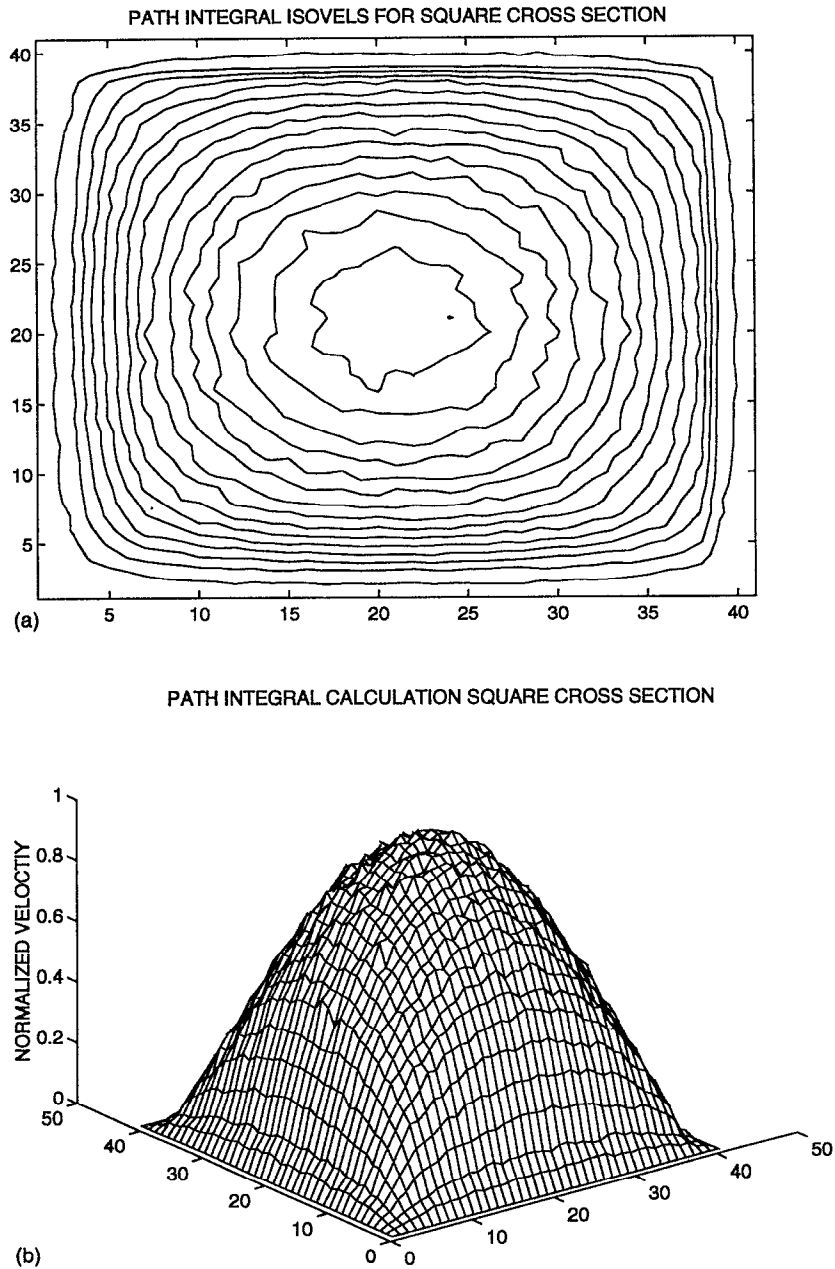


FIG. 1. Velocity fields for a duct having a square cross section calculated by probabilistic method. (a) Lines on the interior of square domain denote isovelocity contours. (b) Magnitude of velocity field for square duct in relief. The velocity field in (b) strongly resembles the experimentally determined velocity field obtained by laser doppler velocimetry (Ref. 31). The average absolute deviation of the numerical results from analytical calculation was 2.4%.

A. Square duct

The rectangular duct is one of the simplest classical geometries for which analytical and experimental results are available.^{7,8} This geometry has also been examined recently to test the accuracy of laser doppler velocimetry as a method of measuring velocity fields.³¹ In Fig. 1 we

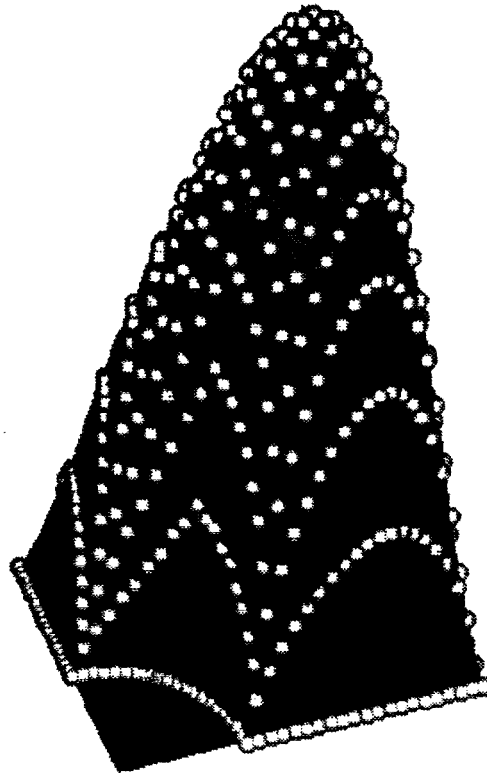


FIG. 2. Velocity field for "notched" duct. The notched duct arises in modeling flow through a duct having periodically placed cylindrical inclusions. The dark region in the left corner corresponds to the inclusion so there is no flow in this region. The dark surface represents the flow velocity field calculated probabilistically while the white circles represent finite element calculations (Ref. 32). The average absolute deviation of the probabilistic and finite element calculations is less than 2%.

show the probabilistic calculation of the velocity field for the rectangular duct where the duct cross section is partitioned into a 40×40 grid. At each interior point 3000 random walks are launched and then stopped either when they reach the boundary of the rectangle or the maximum number of times steps $TMAX=1000$ have been taken. Figure 1(a) shows the isovelocity contours (or isovels) in the square cross section, while Fig. 1(b) shows the velocity field surface with the maximum velocity normalized to equal 1. It is interesting to note that the calculated velocity field (including the mild statistical fluctuations) closely resembles the experimentally determined velocity field in Ref. 31. A comparison with the exact velocity field shows agreement to within an average of 2% at the interior points of the duct.

B. Rectangular duct with round notch

The rectangular duct with a circular notch geometry arises in an injection molding application.³² We will compare the results of our calculation with a numerical solution obtained by the finite element method. 8281 points in the interior were used as initial positions on a rectangular grid with dimensions 0.5×0.6 . In this calculation 2000 walks were performed for each position and the maximum number of steps was $TMAX=40\,000$. The step size in this and the following example in Sec. IV C was $h=0.005$. On comparing with the finite element calculation at 441 points in the interior we found an average absolute error of 1.4%. Figure 2 shows a smoothed

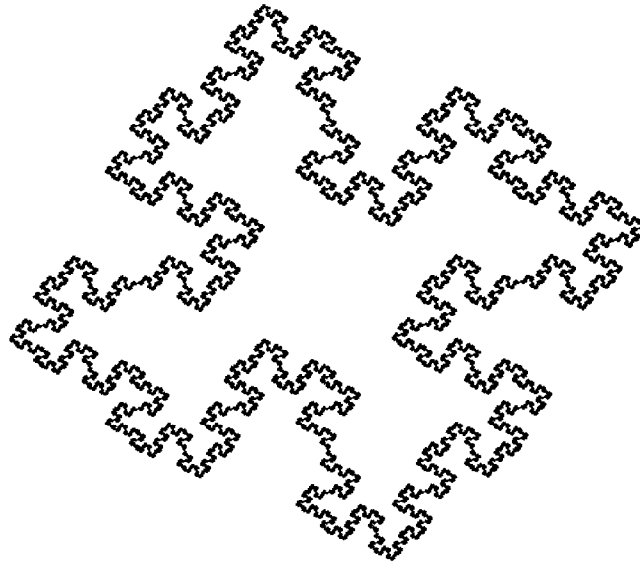


FIG. 3. Boundary of model fractal duct. The choice of boundary shape is motivated by related experimental and theoretical studies of the vibration of a fractal drum having the same shape (Ref. 30).

velocity surface obtained from the Monte Carlo calculation along with the results of the finite element calculation depicted as white balls.

C. Fractal boundary

There has been significant recent interest in the influence of boundary shape on the vibration of membranes.³⁰ It has been suggested that the existence of many fractal-like structures in nature may have their origin in the stabilizing effects of the fractal boundary in damping harmonic excitations.³⁰ Similarly, it is interesting to inquire into the related Poiseuille flow problem to see the influence of the rough boundaries on duct flow.^{6(a)} We now illustrate the results of a Monte Carlo calculation on a fractal “snowflake” shown in Fig. 3. The boundary of this shape consisted of 16 384 points (about 5 generations). 10201 points in the interior of a rectangle containing the shape were used as initial positions of the walk. Figure 4 shows the surface of first-passage times which on suitable normalization is the velocity at each point. The maximum number of steps TMAX was 40 000.

We observe from Fig. 4 that the velocity field qualitatively resembles the fundamental mode in the corresponding drum vibration problem³⁰ and that the rough boundary tends to create a nonmonotone variation of the velocity field from the center of the flow, giving rise to an extended region near the boundary where the flow is slow but nonvanishing. The effect is quite similar to the damping of the membrane motion observed near the boundary in the fractal membrane problem. It seems reasonable to speculate that the reduced shear straining near the boundary could provide a mechanism for the stabilization (and thus formation) of such fractal boundaries in nature. There are classical arguments for the complex branching structures observed in the blood vessels of organisms which are based on the idea of minimizing the dissipation of energy in Poiseuille flow subject to the constraint of the energetic cost of forming the capillary structure.^{33c} The fundamental mode in the fractal drum problem displays interesting mathematical behavior consistent with the physical considerations just described. Very pronounced gradients of the eigenfunction occur near certain points of the boundary. Sapoval first observed this formally and experimentally and discussed their physical implications in similar terms.^{50(c)} Calculation of the drum eigenfunctions for fractal boundaries is a nontrivial problem and these sharp features can be

PATH INTEGRAL CALCULATION FOR FRACTAL CROSS SECTION

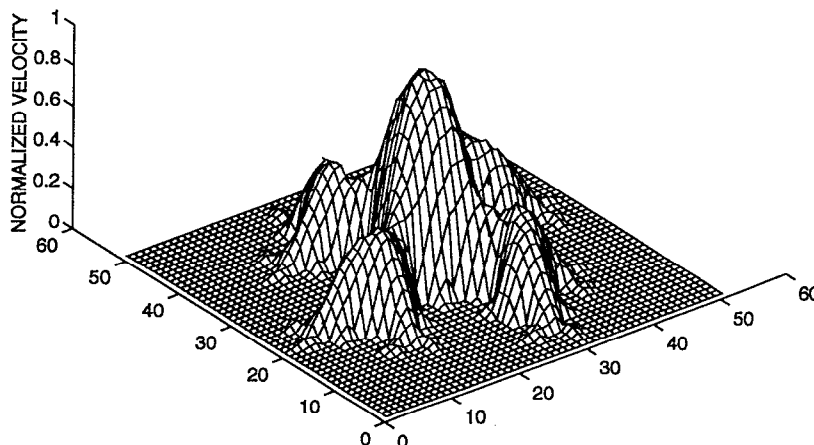


FIG. 4. Probabilistic estimate of the velocity field of a fractal tube. The velocity field corresponds to the tube cross section shown in Fig. 3.

easily missed in an approximate calculation. However, Lapidus and Pang recently proved the existence of points on the boundary of “snowflake” domains where the gradient approaches infinity as the boundary is approached. Their results are in fact valid for a larger class of domains that include the fractal shape we are considering. Lapidus in joint work with Neuberger, Renka, and Griffith computed the gradient of the eigenfunction numerically and found such high gradient points as can be seen in their plotted surface.^{50(b)} We suspect that an analogous phenomenon occurs in our case. One can see that there are spikes near certain points of the boundary. We conjecture that there exists points on the boundary of the fractal snowflake where the gradient of the solution of the Poisson problem approaches infinity. A way to investigate this conjecture is suggested in Appendix A. We also note the related phenomenon of injecting a low viscosity fluid into a viscous medium where the boundary is free to evolve to minimize dissipation. The flow structure often obtains a conspicuously fractal character if injection occurs at a sufficiently high rate. A random walk formulation of this type of flow instability has recently been given.^{33(c)}

There is another application of this type of probabilistic calculation involving a fractal boundary. Duplantier²⁰ has recently shown that the leading term in the electrostatic free energy of a conducting cavity containing electrolyte in the low salt limit is governed by the mean first-passage time averaged over all interior coordinates. These results, which are relevant to the properties of colloid solutions, can be immediately obtained from our algorithm.

D. Special flows

We next consider a special flow involving a nonsimply connected flow space which arises in applications and also a channel flow. Figure 5 shows the calculated isovels of an ideal fiber material in which the circular cylindrical fibers are parallel to the flow direction and are situated on a square lattice within a rectangular channel. No attempt was made to exploit the symmetry of the problem and the local variations in the flow velocity reflect fluctuations in the probabilistic calculations. This was a relatively short calculation (TMAX=1000) with a large random step, $h=0.01$. There were a total of 8281 positions at which random walks were initialized with 800 walks performed at each position. Permeability of 4×4 subsquares of this array were carried out and compared with finite element calculations and agreed to 10%. Observe the interesting topo-

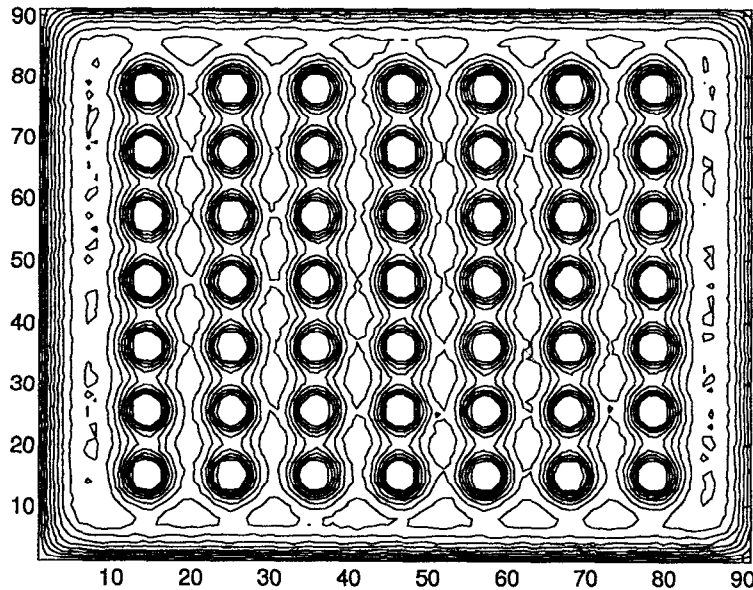


FIG. 5. Flow through tube with cylindrical inclusions. This geometry, which arises in injection molding applications, illustrates a nonsimply connected flow space. The probabilistic calculations of the velocity field reveal interesting changes in topology with changes in the placement and size of the obstructions. These geometric aspects of “screening” deserve further study.

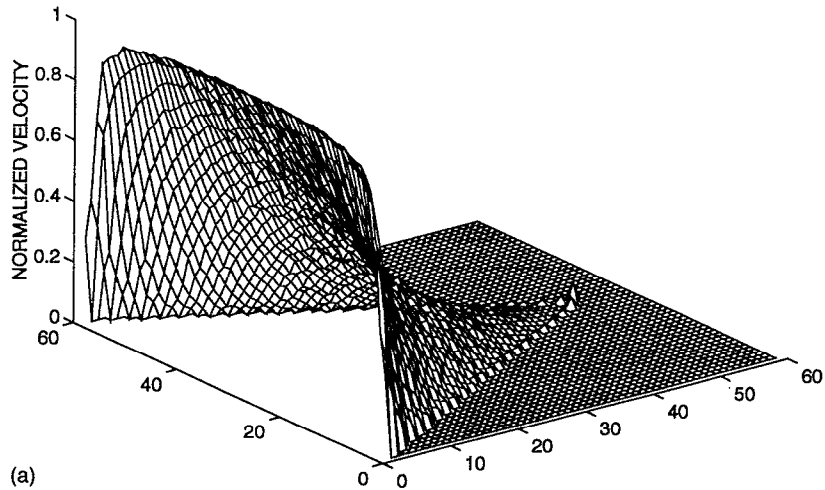
logical structure of the isovels in Fig. 5 which reflect the strong hydrodynamic interaction between the fibers and between the fibers and the walls. Experiments show that small fluctuations in the placement of the fiber plugs can lead to large changes in the flux.³⁴ It would be interesting then to consider fluctuations in the fiber plug placement to investigate the resulting influence on the Poiseuille velocity field and the net flux.

As a final example we consider a channel flow with a free surface exposed to air. We suppose that the idealized free surface is perfectly flat and the channel cross section is uniform as in the duct flow above. At the air surface, the normal derivative of the velocity vanishes (the Neumann boundary condition). This type of flow is important for modeling flow in extruders where the channel is imagined to be wrapped around a cylinder. The probabilistic method can still be applied in this case (see Appendix B for the mathematical argument) by using random walks that reflect back into the interior of the region \mathcal{D} at the air surface boundary.⁷ The results of the calculation for a triangular shaped channel can be seen in Figs. 6(a) and 6(b). Note the enhanced velocity near the air surface.

IV. DISCUSSION

There are many physically important boundary value problems of mathematical physics which can be formulated in terms of integration in the space of continuous functions. In other words, the solution of these problems can be obtained by evaluating some functional of Brownian motion. From the computational point of view this generally means averaging over random walks, the discretized analog Brownian motion. The functionals we are interested in calculating generally involve what are called “stopping times” in probability theory and “first-passage” times in the physical literature. These techniques have been known to researchers in probability theory for decades, and have been used increasingly by scientists in other fields in recent years. With the advent of powerful parallel computational facilities the exploration of these methods for solving problems involving complicated boundaries should be undertaken. Our primary motivation was to

PATH INTEGRAL CALCULATION TRIANGULAR CROSS SECTION



ISOVELS AND VELOCITIES FOR TRIANGULAR CHANNEL AS IN 6A

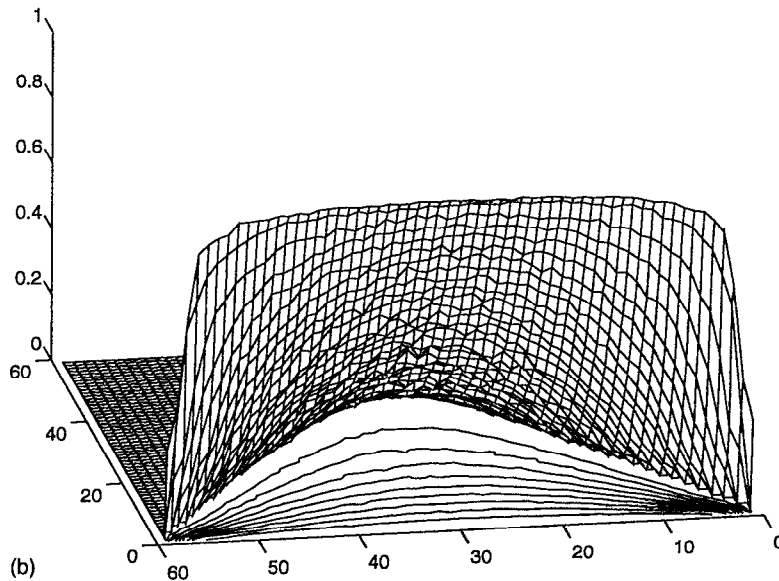


FIG. 6. Velocity field of a triangular duct with a “free” air surface. This type of open-channel flow arises in modeling extruder flow. The probabilistic calculations in (a) show the gradient in the velocity field from the top of the triangular duct. Figure (b) shows the projected “isovel” lines. Notice that the fluid moves much faster at the free air surface. The flux is greatly diminished when the free surface touches a solid boundary. This means that the partially filled extruder will have a much greater flux at the same pressure drop. Many qualitative features of such complex flows can be understood intuitively from the probabilistic algorithm for calculating velocity fields. The increased intuition which comes with this new means of modeling flow should be as important as the capacity of the probabilistic method to treat complex boundaries.

demonstrate the viability of the probabilistic path averaging method. Thus, we consider simple flow geometries (square and notched rectangle) to check the accuracy of the method and more complicated geometries that illustrate its versatility and ease of implementation. For high precision calculations of the velocity field at each point of a cross section with relatively smooth geometry other methods have an advantage, but in complex geometries high precision may be quite difficult to achieve both numerically and experimentally. Quantities of practical interest such as the permeability or flux frequently require lower precision and errors of a few percent will be quite adequate.

The probabilistic averaging technique for Poiseuille flow is shown to give accurate results in test cases. At present the technique sometimes requires long computational times relative to more conventional techniques for simple boundaries. However, we suspect this method is competitive when boundaries are complex and implementation of alternatives becomes time consuming or difficult. We are currently working on improving the computation time and are encouraged by the fact that dramatic reductions in computation time were achieved recently for a similar algorithm that calculates the capacity of objects having complex shape.³⁶ In connection with this work we note that Brownian motion rather than random walks can be used in our algorithm.³⁶

Our calculations of the velocity field of Poiseuille flow for complex-shaped boundaries lead to many interesting results which are independent of the mathematical motivation of the present work discussed above. There are numerous technological problems which can be related to Poisson's equation (1) with Dirichlet boundary conditions and our probabilistic method also provides an algorithm for solving these problems. The illustrative example of a fractal boundary shows the general effect of diminished flow near the rough boundary which complements observation of suppressed vibration near the boundaries of clamped fractal drums. These observations could have an important bearing on the formation of fractal channels in nature which arise under flow conditions where the boundaries are free to adjust to minimize dissipation in flow. The probabilistic calculations for flow through a channel with obstructions also show interesting long range screening effects between the obstructions which are reflected in a changing topology of the isovel lines with position and density of the obstructions. These effects deserve further study and the probabilistic algorithm provides a convenient vehicle for such studies.

Recently, there has been interest^{38,39} in modeling non-Newtonian pipe flow and a generalization of the probabilistic method to describe such flows (which often arise in practice) would be useful. A few speculative remarks on such generalizations are worth mentioning. At high flow rates the flow through a pipe becomes turbulent. Momentum diffusion from the pipe interior to the boundary can be expected to be facilitated by large scale coherent structures in the turbulent fluid.³⁹ Hayot⁴⁰ has generalized the lattice gas approach to tube flow,⁴¹ which recovers the Poiseuille flow when momentum diffusion occurs as a local nearest-neighbor process, to the more spatially erratic momentum diffusion expected in the more turbulent fluid, assumed to occur as a Lévy random walk. This argument is evidently an approximate one, but can be expected to capture salient features of the velocity field of turbulent fluid flow and indeed the lattice gas calculations of Hayot have a qualitative resemblance to observed turbulent flow velocity fields.⁴² We can similarly generalize our algorithm to employ Lévy flight random walks rather than nearest-neighbor random walks. In the case of a circular duct exact analytical results are known for the average first-passage time of the Lévy random walk which illustrate the qualitative effect to be expected for this model of erratic momentum diffusion. For a Lévy flight having index α the average exit time $E_x[\tau]$ for a circle (cross section of a circular duct) equals⁴³

$$E_x[\tau] = N(\alpha, d)(1 - x^2)^{\alpha/2} R^\alpha, \quad (5)$$

where x is the distance from the center of the duct in units of the duct radius R , and $N(\alpha, d)$ is a constant depending on α and on the dimensionality d of the cross section. The usual parabolic profile is recovered in the nearest-neighbor random walk as an approximation to Brownian motion ($\alpha=2$). For the case $\alpha < 2$ we obtain a flattening of the velocity profile associated with increasing

spatial intermittency of momentum diffusion. This qualitative effect is seen in experiments on turbulent pipe flows and in the model lattice gas calculations of Hayot.⁴⁰ Quantitative calculation requires a self-consistent means of calculating the index α . In the meantime we note that comparison of Eq. (5) to the velocity field of high Reynolds number ($Re \approx 10^6$) flow through a circular cross section pipe⁴² [see Fig. 1(D) of Ref. 42] shows agreement to within a few percent when $\alpha = 0.28$. The Lévy flight approach seems very promising from an experimental standpoint. It would be interesting to see if the Lévy flight first-passage time calculations reproduce the unusual velocity fields observed in turbulent flow through noncircular ducts.⁴²

It is also observed that certain complex fluids exhibit deviations from Poiseuille flow even at low flow rates.^{44,45} In polymeric fluids⁴⁶ and suspensions of particles⁴⁶ this effect is often observed. DeGennes⁴⁵ has suggested that flow in polymeric fluids occurs with partial slip rather than the stick boundary condition (2). This view is consistent with the momentum diffusion to the boundary being inefficient due to "entanglement" effects in the polymer fluid. A similar effect might be expected in the particle suspension due to the granularity of the fluid.⁴⁵ Replacing the stick boundary condition in the random walk calculation with a boundary condition in which the random walk is killed with a certain probability,⁴⁶ should lead to a flattening of the velocity field similar to that as observed experimentally. The character of this flattening should be distinctly different than the turbulent fluid case. It remains to be seen whether this approach would lead to a quantitative description of observed non-Newtonian pipe flows, but this model seems worth exploring.

The Poiseuille flow calculations suggest many further generalizations even in cases where slow ("Stokes") flow is an appropriate idealization. Three dimensional ducts with sufficiently smooth axial geometry can be approximated by sequentially piecing together sections with constant cross sections. Assuming the pressure gradient is slowly varying, a solution of Eqs. (1) and (2) for the approximate stack geometry can be computed by requiring that volume fluid flow be conserved across the interface. Geometries to which this can be applied arise in practice. McCauley in Ref. 47 demonstrated that North Sea sandstone rock formations are in good agreement with such an idealized stack model. This method could be used to study flow through porous media of this type.

In conclusion, the probabilistic path averaging method promises to be a versatile tool in hydrodynamic and other technical applications and we have only begun to explore the potentialities of this method.

ACKNOWLEDGMENTS

It is the pleasure to acknowledge the help of Judy Devaney, Howland Fowler, and Holly Rushmeier of the Scientific Computing and Environments Division of NIST. We thank Sridhar Ranganathan for sharing the results of his work with us. We would also like to thank Richard Parnas for preliminary work and encouragement, and Joseph Hubbard, and James Given for helpful discussions.

APPENDIX A: DERIVATION OF ALGORITHM EQUATIONS

The purpose of this section is to discuss the mathematical aspects of our work in a little more detail, first showing the mathematical foundation for the probabilistic algorithm. As we mentioned in the article, these facts are well known to probabilists but may be less well known to others particularly in the discrete time and state space setting of random walks. We will therefore present a brief discussion and derivation for random walks that in the continuous time and state space setting of Markov processes is known as Dynkin's formula. The formula can be interpreted as a path integral representation of the solution of Poisson's equation and our algorithm is essentially a Monte Carlo implementation of it. Our discussion in the article dealt with random walks on a

grid in R^2 but the basic ideas are applicable to random walks on a grid of vectors in R^l , where $\vec{x}=(x_1,x_2,\dots,x_l)$, with $x_i=k_ih$, $k_i \in Z$ and $h>0$ is the distance between neighboring grid points. Any such \vec{x} can be represented as

$$\vec{x}=x_1\vec{e}_1+\dots+x_l\vec{e}_l, \tag{A1}$$

where \vec{e}_i is the vector in R^l whose i th component is 1 and all other components are zero. The set of all vectors satisfying Eq. (A1) will be called H^l . Arrows over the vectors will be dropped in the succeeding discussion. We are interested in the symmetric nearest-neighbor random walk where the probability that a walker situated at x and taking a single step, arrives at y and satisfies

$$p(1,x,y)=\begin{cases} 1/2l, & \text{if } y=x+he_k \text{ for some } k=1\cdots l \\ 0, & \text{otherwise.} \end{cases}$$

Let f be a real valued function defined on H^l . Define the operator P on the set of such functions as

$$Pf(x)=E_x f(x(1))=\sum_{y \in H^l} p(1,x,y)f(y), \tag{A2}$$

where $x(1)$ is the position of the walker after the first step. In view of Eq. (A2) we have

$$Pf(x)=1/2l \sum_{k=-l}^{k=l} f(x+he_k), \tag{A3}$$

where $e_{-n}=-e_n$. Denoting the identity operator by I , we can form $(P-I)/h^2$, a discretization of $\Delta/2$ where Δ is the Laplacian operator. In what follows we can assume without loss of generality that $h=1$. We now seek a solution f of the discretized Poisson equation.

$$(P-I)f(x)=-1 \tag{A4}$$

if $x \in B \subset H^l$ and

$$f(x)=0 \tag{A5}$$

for $x \in \partial B$, with $f:H^l \rightarrow R$ and where ∂B is the set of points not in B that have at least one neighbor in the set B . If $B \subset H^l$ is finite, the existence and uniqueness of f is proven in Ref. 48. The proof for $l \leq 2$ is different and more difficult than the case $l \geq 3$, a reflection of the fundamental difference in the behavior of the random walks in these spaces.

For all dimensions the following properties of the powers of P will be useful. Let $p(n,x,y)$ be the probability that a walker situated at x winds up at y after taking n random walk steps. The so-called Markov property then implies

$$p(n+1,x,y)=\sum_{z \in H^l} p(1,x,z)p(n,z,y).$$

Thus if $P^n f(x) = \sum_{y \in H^l} p(n,x,y)f(y)$ then

$$P^{n+1}f(x)=P \cdot P^n f(x). \tag{A6}$$

It will also be useful to write $P^n f(x) = E_x(f(x(n)))$. As discussed in the text our goal is to relate the first-passage time of a random walk starting in B to the boundary ∂B , denoted by the letter τ , to the solution of Eqs. (A4) and (A5). We will assume that the set $B \cup \partial B$ is finite so that the expected value of τ is finite for all starting points in B .

Let u be an arbitrary bounded function $u: H^l \rightarrow R$. We define the functions ϕ_α , for $0 < \alpha < 1$ as

$$(I - \alpha P)u = \phi_\alpha. \tag{A7}$$

Now u can be written as

$$u(x) = \sum_{n=0}^{\infty} \alpha^n P^n \phi_\alpha(x) = E_x \left(\sum_{n=0}^{\infty} \alpha^n \phi_\alpha(x(n)) \right). \tag{A8}$$

The probabilistic algorithm is based on the following:

Theorem 1:

$$u(x) - E_x \left[\sum_{n=0}^{\tau-1} \alpha^n \phi_\alpha(x(n)) \right] = E_x[\alpha^\tau u(x(\tau))]. \tag{A9}$$

Proof of theorem:

$$E_x \left[\sum_{n=0}^{\infty} \alpha^n \phi_\alpha(x(n)) \right] = E_x \left[\sum_{n=0}^{\tau-1} \alpha^n \phi_\alpha(x(n)) \right] + E_x \left[\sum_{\tau}^{\infty} \alpha^n \phi_\alpha(x(n)) \right] \tag{A10}$$

but

$$E_x \left[\sum_{\tau}^{\infty} \alpha^n \phi_\alpha(x(n)) \right] = E_x \left[\alpha^\tau \sum_{k=0}^{\infty} \alpha^k \phi_\alpha(x(\tau+k)) \right].$$

Since the conditional probability that the path at time $\tau+k$ is at y when the path was at z at time τ satisfies $\text{Prob}\{x(\tau+k) = y | x(\tau) = z\} = p(k, z, y)$

$$E_x[\phi_\alpha(x(\tau+k))] = E_x[E_{x(\tau)}\phi_\alpha(x(k))].$$

We have

$$E_x \left[\sum_{n=\tau}^{\infty} \alpha^n \phi_\alpha(x(n)) \right] = E_x \left[\alpha^\tau \sum_{k=0}^{\infty} E_{x(\tau)}\phi_\alpha(x(k)) \right] = E_x[\alpha^\tau u(x(\tau))].$$

□

Now Eqs. (A9) and (A7) imply that

$$u(x) = E_x \left[\sum_{n=0}^{\tau-1} (I - \alpha P)u(x(n)) \right] + E_x[\alpha^\tau u(x(\tau))]. \tag{A11}$$

We assume $E_x(\tau) < \infty$ for all $x \in B$, so that the limit of Eq. (A11) as $\alpha \rightarrow 1$ is

$$u(x) = E_x \left(\sum_{n=0}^{\tau-1} (I - P)u(x(n)) \right) + E_x(u(x(\tau))). \tag{A12}$$

Noting that any random walk that has exited B must be located in ∂B at time τ , we find on substituting the the solution f of Eqs. (A4) and (A5) for u in the above equation that

$$f(x) = E_x \left[\sum_{n=0}^{\tau-1} 1 \right] = E_x(\tau). \tag{A13}$$

The extension of Theorem 1 to continuous time processes like Brownian motion is accomplished by appealing to the the strong Markov property.

APPENDIX B: REFLECTING BOUNDARY CONDITION

Although example in Sec. III involves a reflecting rather than absorbing boundary condition on one side of the triangle, the probabilistic algorithm still produces a solution of Stokes equation with these boundary conditions. To see this note that when the reflecting boundary of the triangle is extended out to $\pm\infty$, we may now consider reflecting Brownian motion in a wedge of angle π . The work of Varadhan and Williams²⁸ shows that this process has the strong Markov property and hence Dynkin’s formula is valid. We consider τ to be the time the process encounters the two sides of the triangle with absorbing boundary conditions. With this choice, the solution can again be expressed in terms of an average value of time τ as before.

APPENDIX C: POISSON’S EQUATION ON FRACTAL SHAPES

A significant advance in understanding some of the unique properties of the Laplacian operator on irregular boundaries was achieved recently when Lapidus and Pang proved the existence of boundary points where the gradient of the principal eigenfunction tends to infinity, as the boundary point is approached.⁵⁰ The class of domains they considered includes classical fractal shapes. In particular for the Koch snowflake there are an uncountable infinity of such points which can be characterized mathematically. Their result confirms the earlier observations of Sapoval and co-workers who did numerical and experimental investigations of the vibrational modes of fractal drums. It is not known at this point whether a similar property holds for solutions of the Poisson equation but the phenomenon may be investigated by studying the behavior of the variance near the boundary. The variance can be approximated directly from the simulations, so that an estimate of the L^2 average of the gradient along the Brownian motion path is possible without calculating the gradient of the solution itself. Here $\text{Var}(\tau) = E_x[(\tau - E_x(\tau))^2]$. The variance is related to the velocity gradient because of the following:

Theorem 2: *Let B_t be Brownian motion at time t and starting at x an interior point of D , at time $t=0$. If u is the solution of Eq. (1) and τ is the time the path exits D , then*

$$\text{Var}[\tau] = E_x \left(\int_0^\tau |\nabla u(B_t)|^2 dt \right). \tag{C1}$$

The proof of the this theorem is a consequence of some basic results in the theory of stochastic integrals.⁵² One can then compute an average of the gradient as

$$\left(\frac{\text{Var}[\tau]}{E_x[\tau]} \right)^{-1/2}. \tag{C2}$$

We conjecture that boundary points that are near interior points for which Eq. (C2) is large are candidates for the divergent behavior seen in the eigenfunction case. The probabilistic algorithm can be used to detect such divergence and to check the results of other numerical methods.

- ¹(a) F. A. L. Dullien, *Porous Media: Fluid Transport and Pore Structure* (Academic, New York, 1992); (b) A. E. Scheidegger, *The Physics of Flow Through Porous Media* (University of Toronto, Toronto, 1974).
- ²L. M. Schwartz, N. Marty, D. P. Bentz, E. J. Garboczi, and S. Torquato, *Phys. Rev. E* **48**, 4584 (1993). The references of this work provide a good summary of recent contributions to flow through porous media.
- ³(a) R. A. Sampson, *Philos. Trans. R. Soc. A (London)* **182**, 449 (1891); (b) R. Roscoe, *Philos. Mag.* **40**, 338 (1949); (c) F. C. Johansen, *Proc. R. Soc. London, Ser. A* **126**, 231 (1930); (d) H. Hasimoto, *J. Phys. Soc. Jpn.* **13**, 633 (1958); (e) A. M. J. Davis, *J. Fluid Mech.* **231**, 51 (1991).
- ⁴(a) H. S. Keshgi, *Phys. Fluids A* **5**, 2669 (1993); (b) R. M. Tirrill, *ibid.* **29**, 2351 (1986); (c) C. Y. Wang, *ibid.* **5**, 1113 (1993); (d) K. B. Ranger, *ibid. A* **5**, 3029 (1993).
- ⁵(a) I. G. Wilson, *Nature* **241**, 393 (1973); (b) S. Kramer and M. Marder, *Phys. Rev. Lett.* **68**, 205 (1992); (c) R. A. Callander, *J. Fluid Mech.* **36**, 465 (1969); (d) G. Parker, *ibid.* **89**, 109 (1978).
- ⁶(a) J. F. Douglas and A. Friedman, in *Mathematics in Industrial Problems* (Springer-Verlag, New York, 1994), part 7, p. 166; (b) J. F. Douglas, H. X. Zhou, and J. B. Hubbard, *Phys. Rev. E* **49**, 5319 (1994).
- ⁷(a) J. G. Butcher, *Proc. London Math. Soc.* **8**, 117 (1876); (b) A. G. Greenhill, *ibid.* **13**, 48 (1881); (c) O. Heaviside, *Philos. Mag.* **23**, 10 (1887).
- ⁸(a) J. Happel and H. Brenner, *Low Reynolds Number Hydrodynamics* (Prentice Hall, Englewood Cliffs, NJ, 1965); (b) H. Brenner, *ZAMP* **32**, 347 (1981).
- ⁹H. L. Weissberg, *Phys. Fluids* **5**, 1033 (1962).
- ¹⁰R. W. Penn and E. A. Kearsley, *J. Res. Natl. Bur. Stand. A* **75**, 553 (1971).
- ¹¹Z. Shi-Xing and W. Zhi-Qing, *Appl. Math. and Mech. (China)* **14**, 837 (1993).
- ¹²J. B. Diaz and A. Weinstein, *Am. J. Math.* **70**, 107 (1948). St. Venant's torsion problem is related to the Poiseuille flow problem for rods and tubes, respectively, having arbitrary simply connected cross section (14b).
- ¹³(a) T. J. Higgins, *Am. J. Phys.* **10**, 248 (1942); *J. Appl. Phys.* **14**, 469 (1943); *Proc. Soc. Exptl. Stress Anal.* **2**, 17 (1945); (b) W. Thomson, *Mathematical and Physical Papers* (Clay and Sons, London, 1890), Vol. 3, pp. 57–65.
- ¹⁴(a) G. Pólya, *Q. Appl. Math.* **6**, 267 (1948); *J. Ind. Math. Soc.* **24**, 413 (1960); (b) G. Pólya and G. Szegő, *Isoperimetric Inequalities in Mathematical Physics* (Princeton University, Princeton, 1951); (c) L. E. Payne and H. F. Weinberger, *J. Math. Anal.* **2**, 210 (1961); (d) E. Makai, *Acta Math. Acad. Sci. Hungary* **17**, 419 (1966); (e) L. E. Payne, *SIAM Rev.* **9**, 453 (1967); (f) L. E. Payne and G. A. Philippin, *SIAM J. Math. Anal.* **14**, 1154 (1983); (g) J. L. Synge, *Proc. Sym. Appl. Math.* (McGraw-Hill, New York, 1953), Vol. 4, p. 141; (h) G. Pólya and A. Weinstein, *Annals. Math.* **52**, 154 (1950).
- ¹⁵(a) S. Timoshenko, *Proc. London Math. Soc.* **20**, 389; 398 (1922); (b) J. Cornish, *Proc. R. Soc. London, Ser. A* **120**, 691 (1928); (c) I. S. Sokolnikov, *Trans. Am. Math. Soc.* **33**, 719 (1931); (d) W. J. Duncan, *Proc. R. Soc. London, Ser. A* **136**, 95 (1932); (e) N. M. Basu, *Philos. Mag.* **10**, 886 (1930); **10**, 896 (1930); (f) P. M. Quinlan, *Proc. R. Soc. London, Ser. A* **282**, 208 (1964); (g) R. Courant, *Bull. Am. Math. Soc.* **49**, 1 (1943).
- ¹⁶(a) D. G. Christopherson and R. V. Southwell, *Proc. R. Soc. London, Ser. A* **168**, 317 (1938); (b) K. N. E. Bradford, S. G. Hooker, and R. V. Southwell, *Proc. R. Soc. London, Ser. A* **159**, 315 (1937); (c) R. Weller, G. H. Shortley, and B. Fried, *J. Appl. Phys.* **11**, 283 (1940); (d) R. M. Morris, *Math. Ann.* **116**, 374 (1939); **117**, 31 (1939); *Proc. Lond. Math. Soc.* **46**, 81 (1941); (e) J. L. Synge, *The Hypercircle in Mathematical Physics* (Cambridge University, Cambridge, 1957), Chap. 4.
- ¹⁷(a) L. Prandtl, *Phys. Z.* **4**, 758 (1902); (b) A. A. Griffith and G. I. Taylor, "The Use of Soap Films in Solving Torsion Problems," in *The Scientific Papers of G. I. Taylor*, edited by G. K. Batchelor (Cambridge University, Cambridge, 1958), Vol. 1, p. 1; (c) B. Johnson, *Civil Eng.* **5**, 698 (1935).
- ¹⁸W. Prager, *De Ingenieur* **48**, 141 (1955).
- ¹⁹(a) W. Schumann, *Q. Appl. Math.* **16**, 309 (1958); (b) J. Leavitt and P. Ungar, *Commun. Pure Appl. Math.* **15**, 35 (1962).
- ²⁰B. Duplantier, *Phys. Rev. Lett.* **66**, 1555 (1991). See Eq. (4) which relates Eqs. (1) and (2) to the first passage-time variable discussed by Duplantier.
- ²¹(a) R. Reck and S. Prager, *J. Chem. Phys.* **42**, 3027 (1965); (b) J. Rubenstein and S. Torquato, *ibid.* **88**, 6540 (1980); (c) S. Torquato, *J. Stat. Phys.* **65**, 1173 (1991).
- ²²D. Y. Kasture, *Q. Appl. Math.* **49**, 635 (1991).
- ²³(a) R. Courant, "Über Partial Differenzengleichungen," *Atti Congr. Int. Mat. Bologna* **3**, 83 (1928); (b) R. Courant, K. Friedrichs, and H. Lewy, *Math. Annal.* **100**, 32 (1928); (Engl. Transl.) *IBM J. Res. Dev.* **11**, 215 (1967); (c) W. H. McCrea and F. J. W. Whipple, *Proc. Roy. Soc. Edinburgh* **55**, 281 (1941); (d) H. Davies, *Q. J. Math.* **6**, 232 (1955); (e) E. M. Keberle and G. Montet, *J. Math. Anal. Appl.* **6**, 1 (1963); (f) G. L. Montet, *J. Math. Phys.* **5**, 1555 (1964); (g) R. J. Duffin, *Duke Math. J.* **20**, 233 (1953).
- ²⁴(a) S. Kakutani, *Proc. Imp. Acad. (Tokyo)* **20**, 706 (1944); **21**, (1945). Kakutani's solution of the interior Dirichlet problem for the Laplace equation, corresponding to arbitrary boundary shape, involves launching random walks from points x interior to the domain D and letting the walks wander until they hit the boundary, as in Wasow's algorithm for solving the Poisson equation (Ref. 25). Solution of the Laplace equation at x , however, involves averaging over the boundary values encountered by the walks initiating from x rather than averaging first-passage times. The Poisson equation (1.1) can be transformed [J. Boussinesq, *J. Math.* **6**, 177 (1880); see also Refs. 8 and 14(e)] in two dimensions

- into the Laplace equation with Dirichlet-type boundary data so that Kakutani's algorithm provides an alternative probabilistic route for calculating Poiseuille flow velocity fields; (b) M. Donsker and M. Kac, *J. Res. Natl. Res. Bur. Stand.* **44**, 581, (1950).
- ²⁵ (a) W. Wasow, *J. Research NBS* **46**, 462 (1951); (b) See Ref. 8(b) for a discussion of Poiseuille Flow in d dimensions which should be compared to Wasow's first passage time calculations in d dimensions.
- ²⁶ (a) I. C. Kim and S. Torquato, *J. Appl. Phys.* **69**, 2280 (1991); (b) see Refs. 21(b)–21(c); (c) J. Tobochnik, *Comput. in Phys.* **4**, 181 (1990).
- ²⁷ (a) S. Torquato, *Phys. Rev. Lett.* **64**, 2644 (1990); (b) M. Avellaneda and S. Torquato, *Phys. Fluids A* **3**, 2529 (1991).
- ²⁸ J. Bernal, NIST Technical Note 1252 (1988).
- ²⁹ (a) P. M. Adler, *Phys. Fluids A* **29**, 15 (1985); (b) J. Salles, J. F. Thouvert, R. Delannay, L. Prevors, J. L. Auriault, and P. Adler, *Phys. Fluids A* **5**, 2348 (1993).
- ³⁰ (a) I. Peterson, *Sci. News* **146**, 184 (1993). (b) B. Sapoval, T. Gobron, and A. Margolina, *Phys. Rev. Lett.* **67**, 2974 (1991).
- ³¹ C. E. Camp, W. B. Kolb, K. I. Sublette, and R. L. Cerro, *Exp. Fluids* **10**, 87 (1990).
- ³² F. R. Phelan, Y. Lennig, and R. S. Parnas, *J. Thermoplastic Composite Math.* **7**, 208 (1994).
- ³³ (a) C. D. Murray, *Proc. Natl. Acad. Sci.* **12**, 207 (1926); (b) M. Labarbera, *Contemp. Math.* **141**, 565 (1993); *Science* **249**, 992 (1990); (c) S. Liang, *Phys. Rev. A* **33**, 2663 (1986).
- ³⁴ S. Ranganathan, G. M. Wise, F. R. Phelan, Jr., R. S. Parnas, and S. G. Advani, "A Numerical and Experimental Study of the Permeability of Fiber Preforms," *Proc. 10th Ann. ASM/ESD Advanced Composites Conference and Exposition* (to appear).
- ³⁵ (a) M. Kac, *Probability and Related Topics in Physical Sciences* (Interscience, New York, 1959); (b) M. Rosenblatt, *Trans. Am. Math. Soc.* **71**, 120 (1951).
- ³⁶ J. Given, J. Hubbard, J. Douglas, and H. Zhou, "A First-Passage Algorithm for the Calculation of Capacitance Hydrodynamic Friction and Diffusion-Limited Reaction Rate," preprint.
- ³⁷ B. C. Eu, *Am. J. Phys.* **58**, (1990).
- ³⁸ P. G. De Gennes, *J. Phys. (Paris)* **40**, 783 (1979).
- ³⁹ (a) A. Vincent and M. Meneguzzi, *J. Fluid Mech.* **225**, 1 (1991); (b) P. G. Saffman, *Ann. Rev. Fluid Mech.* **11**, 95 (1979); (c) H. Tennekes, *Phys. Fluids* **11**, 669 (1968); (d) S. Douady, Y. Couder, and M. Brachet, *Phys. Rev. Lett.* **67**, 983 (1991).
- ⁴⁰ F. Hayot, *Phys. Rev. A* **43**, 806 (1991).
- ⁴¹ D. D'Humieres and P. Lallemand, *Physics A* **140**, 326 (1986).
- ⁴² (a) H. Schlichting, *Boundary Layer Theory* (Pergamon, New York, 1955), Chaps. 19 and 20; (b) D. C. Bogue and A. B. Metzner, *Ind. Eng. Chem. Fund.* **2**, 143 (1963).
- ⁴³ R. K. Getoor, *Trans. Am. Math. Soc.* **101**, 75 (1961). The flux from Eq. (5) scales as $R^{d+\alpha-1}$ which could be tested experimentally.
- ⁴⁴ (a) A. Karnis, H. L. Goldsmith, and S. G. Mason, *J. Coll. Int. Sci.* **22**, 531 (1966); (b) H. E. H. Meijer and C. P. J. M. Verbraak, *Polym. Eng. Sci.* **28**, 758 (1988).
- ⁴⁵ (a) P. G. de Gennes, *C. R. Acad. Sci. B* **288**, 219 (1979); (b) K. B. Migler, H. Herret, and L. Leger, *Phys. Rev. Lett.* **70**, 287 (1993); (c) L. DeVargas and O. Manero, *Polym. Eng. Sci.* **29**, 1232 (1989).
- ⁴⁶ The partial killing random walk boundary condition corresponds in the Laplace or diffusion equations to a "radiative" boundary condition. We suspect this is also true for the Poisson equation but we can only demonstrate this connection in the "absorbing" ("Dirichlet") and "reflecting" ("Neumann") boundary condition limits of the radiative boundary condition. [See G. H. Weiss, *Aspects and Applications of the Random Walk* (North-Holland, New York, 1994), Chap. 5]. Intuitively, we identify the mixed stick-slip boundary condition in the hydrodynamic flow problem with the radiative boundary in the diffusion equation as suggested previously by Burgers [*Second report on Viscosity and Plasticity* (North-Holland, New York, 1938), Chap. 3] and this hypothetical relation motivated our partial-killing boundary condition modeling of the partial-slip tube flow in non-Newtonian fluids. Further investigation on these connections between hydrodynamics and diffusion would be useful for future numerical calculation.
- ⁴⁷ J. McCauley, *Physica A* **197**, 528 (1993).
- ⁴⁸ F. Spitzer, *Principles of Random Walk*, 2nd ed. (Springer-Verlag, New York, 1976).
- ⁴⁹ S. Varadhan and D. Williams, *Commun. Pure Appl. Math.* **38**, 405 (1984).
- ⁵⁰ (a) M. Lapidus and M. Pang, *Commun. Math. Phys.* (preprint); (b) I. Peterson, *Sci. News*, **146**, 184 (1994); (c) B. Sapoval, *Physica D* **38**, 296 (1989).
- ⁵¹ M. L. Lapidus, J. W. Neuberger, R. Renka, and C. A. Griffith (preprint).
- ⁵² A. Friedman, *Stochastic Differential Equations and Applications* (Academic, New York, 1975), Vol. 1.